Evidence of Localized Wave Transmission

Richard W. Ziolkowski and D. Kent Lewis
University of California, Lawrence Livermore National Laboratory, Livermore, California 94550

Bill D. Cook
Cullen College of Engineering, University of Houston, Houston, Texas 77204-4792
(Received 5 August 1988)

The feasibility of launching an acoustic directed energy pulse train was tested experimentally. Excellent agreement between theoretical and experimental results was obtained.

PACS numbers: 43.35.+d, 03.40.Kf, 43.20.+g

We report experimental measurements that confirm the existence of acoustic directed energy pulse trains (ADEPT's) for ultrasonic waves in water. These pulses exhibit localized transmission of wave energy. They are generated by a synthetic line array and are detected by a pseudopoint receiver. The measurement technique yields both the amplitude and phase of the pressure field as a function of time.

The possibility of solutions of the scalar wave equation and Maxwell's equations that describe localized, slowly decaying transmission of energy in space-time has been suggested by several groups in recent years. These include exact pulse solutions (focus wave modes,[1,2] electromagnetic directed energy pulse trains,[3,4] splash modes,[5] transient beams[6]), continuous-wave modes (Bessel beams[7]), and asymptotic fields (electromagnetic missiles,[8] electromagnetic bullets,[9] Gaussian wave packets[10]).

ADEPT's are exact pulse solutions of the acoustic (scalar) wave equation in an isotropic, homogeneous medium. They can be constructed from "focus wave modes"[1]; the latter are *exact* solutions that present Gaussian beams translating through space with only local deformations. If c is the propagation speed of waves in this medium, the axisymmetric solution ($\rho^2=x^2+y^2$)

$$\Phi_k(\mathbf{r},t)=e^{ik(z+ct)}\frac{\exp\{-k\rho^2/[z_0+i(z-ct)]\}}{4\pi i[z_0+i(z-ct)]} \tag{1}$$

is a moving, Gaussian pulse modulated by a plane wave. It can have either a plane wave or a particlelike character depending on whether k is small or large.[3] An added degree of freedom has been introduced into the solution through the various k, and these fundamental Gaussian pulse fields can be used as basis functions to represent new transient solutions of the wave equation. In particular, if

$$s(\rho,z,t)=\rho^2/[z_0+i(z-ct)]-i(z+ct),$$

the function

$$f(\mathbf{r},t)=\int_0^\infty \Phi_k(\mathbf{r},t)F(k)\,dk=\frac{1}{4\pi i[z_0+i(z-ct)]}\int_0^\infty dk\,F(k)e^{-ks(\rho,z,t)} \tag{2}$$

is also an exact source-free solution of the wave equation. This representation, in contrast to plane-wave decompositions, uses basis functions that are localized in space and hence, by their very nature, are a natural basis for the synthesis of finite-energy pulse solutions that can be tailored to give directed wave energy transfer in space.[3] These exact, scalar wave equation solutions can also be decomposed into bidirectional, forward and backward, traveling plane-wave solutions.[4] This bidirectional representation is actually a generalization of (2); and like (2), it is complete and has a well defined inverse. It also leads to analogous solutions in geometries with boundaries.[11]

A particularly interesting spectral function is

$$F(k)=4\pi i\beta(\beta k-b)^{\alpha-1}e^{-\alpha(\beta k-b)}H(k-b/\beta)/\Gamma(\alpha),$$

which is derived by the scaling and truncating of a power spectrum. $H(x)$ is Heaviside's function; $\Gamma(x)$ is the gamma function. This choice of spectrum leads to the modified-power-spectrum (MPS) pulse[3]

$$f(\mathbf{r},t)=\mathrm{Re}\left[\frac{1}{z_0+i(z-ct)}\,\frac{1}{(s/\beta+a)^\alpha}e^{-bs/\beta}\right]. \tag{3}$$

For a distance $z\ll\beta/2b$ and $z<\beta a/2$, the amplitude of the pulse at the pulse center is constant; it then becomes oscillatory with an oscillation length of $\pi\beta/b$ in an intermediate zone, $\beta/2b<z<\beta a/2$. The initial amplitude of the MPS pulse is recovered when $z=n(\pi\beta/b)$, n being any positive integer, until the distance $z\sim\beta a/2$; since β is a free parameter, this distance can be made arbitrarily large. When the observation point is far from the origin $z>\beta a/2$, the MPS pulse decays as $1/z^\alpha$. Because the transverse behavior of this MPS pulse at the pulse center

is essentially

$$f(\rho,z=ct)\sim e^{-b\rho^2/\beta z_0} f(\rho=0,\, z=ct)\,,$$

one can adjust the degree of localization transversely by adjusting the ratio $b/\beta z_0$. The MPS pulse is also localized longitudinally, decaying along z as $f\sim 1/[z_0^2+(z-ct)^2]$ away from the pulse center.

Consider, for instance, the MPS pulse with $a=1.0$ m, $\alpha=1.0$, $b=600.0$ m^{-1}, $\beta=300.0$, and $z_0=4.5\times10^{-4}$ m. The value at the pulse center remains constant until about $z\sim\beta/2b=0.25$ m, where it begins to oscillate, recovering its initial amplitude every $\Delta z=1.571$ m until $z\sim\beta a/2=150.0$ m, where the $1/z$ behavior begins to dominate. The $1/e$ point of the amplitude of the pulse in the pulse center cross section $z=ct$ is $\rho=(\beta z_0/b)^{1/2}=1.50$ cm. The frequency spectrum of this pulse in water having a sound speed of 1.5×10^3 m/s has all of its energy below 2.0 MHz. The Rayleigh length (distance to the near-far-field boundary) for a conventional cw, zeroth-order, symmetric Hermite-Gaussian pulse with a waist w_0 at $z=0$ is $L_R=\pi w_0^2/\lambda$. If its frequency is taken to be 2.0 MHz, its wavelength in water is $\lambda=0.075$ cm and $L_R=94.25$ cm. At $z=1.5\times10^4$ cm, the waist of the Gaussian beam would spread to $z\lambda/\pi w_0=238.73$ cm and its amplitude would have decreased by $[1+(\lambda z/\pi w_0^2)^2]^{-1/2}=6.28\times10^{-3}$. The localization of the MPS pulse near the z axis (waist ~1.5 cm at $z\sim1.5\times10^4$ cm) and the recovery of its initial amplitude well beyond the classical far-field distance (amplitude ~1.0 at $z\sim1.5\times10^4$ cm) confirms the improved transmission of energy by the ADEPT's over conventional diffraction-limited beams. The question of practical realization of this result has been addressed numerically and through the following experiment.

The virtue of the ADEPT's is their intrinsic space-time nature. They can be recovered approximately from a finite array of radiating elements by specification of both their spatial *and* their temporal distributions. In particular, a Huygens' reconstruction based on the casual, time-retarded Green's function and a finite planar array of point sources reproduces the MPS pulses at large distances from the array.[3] The driving functions for the array elements are determined by the exact solution f and its derivatives. The point-source representation is also a reasonable approximation to an array of extended sources (such as the acoustic transducers used in the experiment) if the far field of each radiator is reached much before the total field response of the array is measured. The array-generated MPS pulse appears to be very robust and insensitive to perturbations in the initial aperture distributions. These results are also insensitive to the type of array (circular, rectangular, or hexagonal) considered.

The following is a straightforward approach to determine experimentally the feasibility of launching an acoustic MPS pulse facsimile. After comparison to the experimental results and the simulations, the analysis has indicated improvements that will be checked with future experiments.

The radiation experiment is based on ultrasonic pulses propagating in water. The ADEPT parameters are the ones given above. This frequency selection coupled with the choice of array and array element size permits the desired effects to occur in a distance less than 2.0 m, the effective length of our water tank.

Our experimental array is one dimensional, synthetic, and uses reciprocity to reverse the roles of sender and receiver. Consider a conventional array. It would contain multiple elements, infinitely long or at least long enough for the array to be considered one dimensional. Each element of the array needs to be driven simultaneously and would radiate a different function depending on its position in the array. On the other hand, all elements of the synthetic array need not exist simultaneously; one element will suffice. For each position of the receiver, a time history of the received pulse is recorded for each element uniquely excited. These sets of time histories are summed to yield the radiation of the array.

Another aspect of unconventionality of our array-receiver system is the interchange of roles of sender and receiver. Because of reciprocity, the same time response will occur when the roles are reversed. Unlike the disk-to-disk case, the line element case gives no differentiation of the elastic wave field as a result of propagation.[12] In our case the line element is a laser beam. Our sound system consists of a single commercial ultrasonic transducer designed for nondestructive testing for a sender, a low-power laser and photodiode detector as a receiver, and a computer-controlled positioning device. The transducer, which consists of a $\frac{1}{4}$-in. (6.2-mm) diameter circular piezoelectric disk and acoustically matched damping material on its backside, produces a pistonlike motion in the water. Past 6.0 cm, the resulting sound beam is in the far field of the transducer. For a transducer whose resonant frequency is well above the driving spectrum, the velocity of the radiating surface is proportional to the time derivative of the applied electrical signal from the power amplifier. The laser beam is perpendicular to the sound propagation direction. The laser beam passes through the sound field to strike a photodiode. A lens placed between the sound field (exterior to the water tank) and the photodiode effectively positions a virtual image of the photodiode within the tank near the sound field. The optical setup also reduces the size of the virtual photodetector. The photodiode provides an electrical signal that yields the line element response.

The transducer produces a pressure sound field which in turn produces a local variation of the optical refractive index. At the low ultrasonic frequencies of our design, the total optical effect reduces to only a phase modulation occurring at a unique plane within the sound beam.[13,14] The photodetector is not placed in the focal

region but very close to this plane of phase modulation. The magnitude of the phase modulation is the effective optical path length through the local variations of refractive index.[15] For a limited region of propagation, the intensity of the light is proportional to both the distance from the phase plane and the curvature of the wave fronts. The curvature of the wave front is the second derivative of the phase modulation. Thus, for a time signal applied to the ultrasonic transducer a retarded time signal occurs at the photodetector; this signal is proportional to the second time derivative of the spatial line integral of the acoustic pressure along a line defined by the laser beam. Applying the principle of reciprocity, one can interpret this time signal as the response of a circular receiver in the field to an element in the appropriately driven line array. Within the approximations of our design, it is the third derivative (one from the transducer and two from the optics) of the driving function convolved with line-to-disk radiative term.

Let the linear array of experimental element positions be along the y axis, the laser measurement be taken along the x axis, and the direction of propagation be along the z axis. The synthetic linear array consisted of 21 element positions symmetrically arranged about $y=0$ with a 3.0-mm separation. Thus, eleven driving functions were employed, and the total array width was 6.0 cm. The envelope of the frequency spectra of the driving functions is peaked approximately at 0.6 MHz and has 98.0% of its energy below 2.0 MHz. Time records of length 10.24 μs were taken. The 176 unique experimental waveforms, launched with a normalized-to-one maximum amplitude, were weighed and superposed to construct the field of our synthetic linear array. As a control, a Gaussian beam from the same array was constructed with different weights but the same waveform from all array elements. In particular, each element of that array was driven with the center ADEPT driving function and was weighted with a Gaussian amplitude $\exp(-\rho^2/w_0^2)$, where $w_0=1.5$ cm, the same transverse waist at $z=ct=0$ as the ADEPT. For both the experimental Gaussian control and the corresponding numerical simulations, a Gaussian beam field was fitted to the data. The amplitude decay and the beam width resulted from an effective frequency of 0.6 MHz ($\lambda=0.25$ cm), the peak of the spectra of the driving waveforms. The effective Rayleigh length for the experiment was thus $L_R=28.27$ cm.

The energy density of the field measured at 25.0 cm $\sim L_R$ is shown in the upper left-hand panel of Fig. 1. The horizontal axes in Fig. 1 represent 2.56 μs in time or

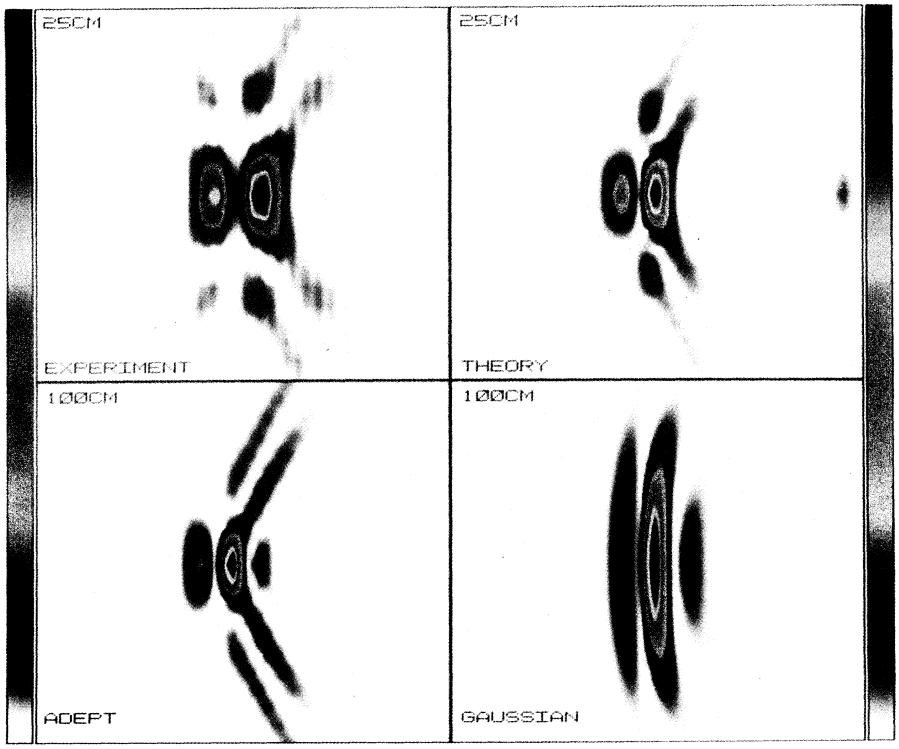

FIG. 1. Upper left-hand panel: Experimental reconstruction at $z=25$ cm of an ADEPT launched from a linear synthetic array. Upper right-hand panel: Theoretical reconstruction at $z=25$ cm of an ADEPT launched from a linear synthetic array. Lower left-hand panel: Field generated at $z=100$ cm from an ADEPT driven, 441 element, 6.0×6.0-cm^2 square array. Lower right-hand panel: Field generated at $z=100$ cm from an Gaussian driven, 441 element, 6.0×6.0-cm^2 square array.

equivalently 0.384 cm, the vertical scales represent -3.0 to $+3.0$ cm. Time increases from left to right. The peak values have been normalized to a maximum of 1.0. The yellow band is approximately 30% down from the peak amplitude; the green band $\sim 45\%$; the light blue band $\sim 60\%$; and the light purple band $> 90\%$. The synthetic linear array experiment is simulated by our driving each element at (x,y) in a rectangular array with the wave function at $(0,y)$. This ensures that the array appears "linear," as does the reciprocal laser diagnostic system. The simulated array is 6.0×6.0 cm^2 and contains 441 elements in a 21×21 equally spaced pattern. Three derivatives of the reconstructed ADEPT are taken to simulate the effects of the diagnostic system. The amplitude of the resulting field is shown in the upper right-hand panel of Fig. 1. Similar agreement is obtained for the simulated and experimental Gaussian-driven arrays.

We found both experimentally and numerically that the linear array produced fields that began to break up after 50.0 cm $\sim 2L_R$. For the rectangular array-generated ADEPT, the nonaxis elements compensate against any splitting. The normalized energy density at $z = 100.0$ cm $\sim 3L_R$ of three derivatives of the theoretical ADEPT ($|\partial_t^3 f|^2$) that is launched from a 6.0-cm square, 21×21 array is shown in the lower left-hand panel of Fig. 1. For comparison with a more conventional pulse, the normalized energy density of three derivatives of the field generated by the Gaussian-driven array is shown in the lower right-hand panel of Fig. 1. At this distance the Gaussian has spread to about 2.75 times its width at 25.0 cm while the ADEPT width has remained essentially the same. With a more complicated set of driving functions, such as the proposed folded array,[3] the ADEPT can be maintained well beyond 10.0 m.

This work was performed in part by the Lawrence Livermore National Laboratory under the auspices of the U.S. Department of Energy under Contract No. W-7405-ENG-48.

[1]J. B. Brittingham, J. Appl. Phys. **54**, 1179 (1983).

[2]R. W. Ziolkowski, J. Math. Phys. **26**, 861 (1985).

[3]R. W. Ziolkowski, in *Microwave and Particle Beam Sources and Propagation,* edited by N. Rostoker, SPIE Conference Proceedings No. 873 (SPIE, Bellingham, WA, 1988), and Phys. Rev. A (to be published).

[4]I. M. Besieris, A. M. Shaarawi, and R. W. Ziolkowski, J. Math. Phys. (to be published).

[5]P. Hillion, J. Appl. Phys. **60**, 2981 (1986), and J. Math. Phys. **28**, 1743 (1987).

[6]E. Heyman and L. B. Felsen, IEEE Trans. Antennas Propag. **34**, 1062 (1986); E. Heyman and B. Z. Steinberg, J. Opt. Soc. Am. A **4**, 473 (1987); E. Heyman, B. Z. Steinberg, and L. P. Felsen, J. Opt. Soc. Am. A **4**, 2081 (1987).

[7]J. Durnin, J. Opt. Soc. Am. A **4**, 651 (1987); J. Durnin, J. J. Miceli, Jr., and J. H. Eberly, Phys. Rev. Lett. **58**, 1499 (1987).

[8]T. T. Wu, J. Appl. Phys. **57**, 2370 (1985); T. T. Wu, R. W. P. King, and H.-M. Shen, J. Appl. Phys. **62**, 4036 (1987); H.-M. Shen, in *Microwave and Particle Beam Sources and Propagation,* edited by N. Rostoker, SPIE Conference Proceedings No. 873 (SPIE, Bellingham, WA, 1988).

[9]H. E. Moses, J. Math. Phys. **25**, 1905 (1984); H. E. Moses and R. T. Prosser, IEEE Trans. Antennas Propag. **34**, 188 (1986).

[10]A. N. Norris, B. S. White, and J. R. Schrieffer, Proc. Roy. Soc. London A **412**, 93 (1987).

[11]A. M. Shaarawi, I. M. Besieris, and R. W. Ziolkowski, J. Appl. Phys. (to be published).

[12]B. D. Cook and D. K. Lewis, in *Proceedings of the Ultrasonics International '87 Conference, London, United Kingdom, July, 1987* (Butterworths, Stoneham, MA, 1987).

[13]E. A. Hiedemann and M. A. Breazeale, J. Opt. Soc. Am. **49**, 372 (1959).

[14]B. D. Cook, J. Opt. Soc. Am. **53**, 429 (1963).

[15]B. D. Cook, J. Acoust. Soc. Am. **60**, 95 (1979).

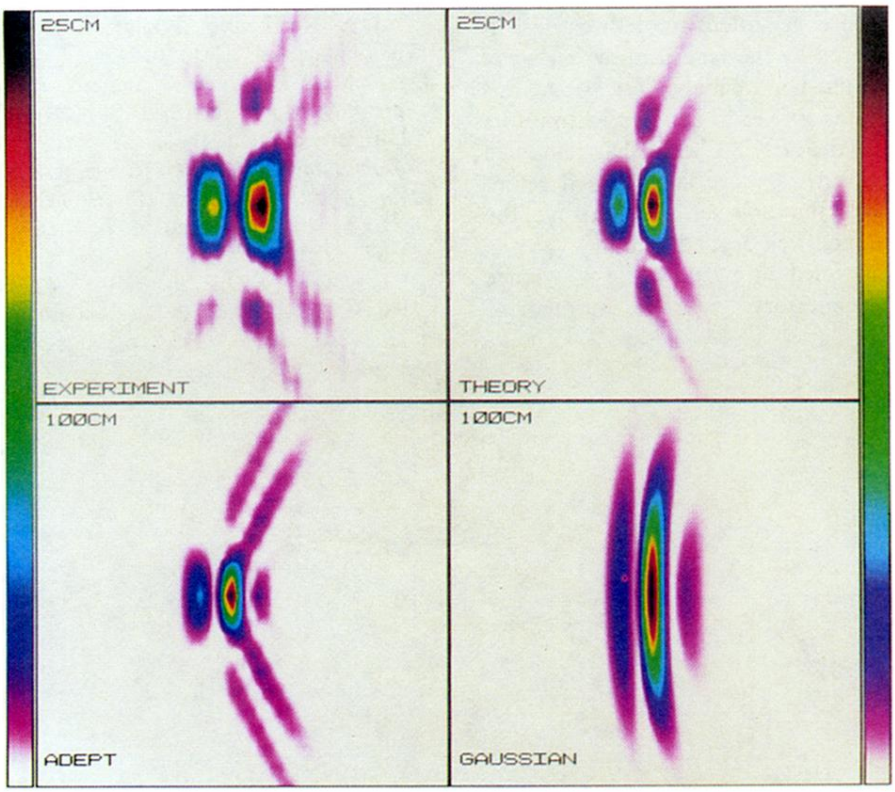

FIG. 1. Upper left-hand panel: Experimental reconstruction at $z=25$ cm of an ADEPT launched from a linear synthetic array. Upper right-hand panel: Theoretical reconstruction at $z=25$ cm of an ADEPT launched from a linear synthetic array. Lower left-hand panel: Field generated at $z=100$ cm from an ADEPT driven, 441 element, 6.0×6.0-cm^2 square array. Lower right-hand panel: Field generated at $z=100$ cm from an Gaussian driven, 441 element, 6.0×6.0-cm^2 square array.